

Development and Performance of the PHOT (Portable High-Speed Occultation Telescope) Systems

E. F. YOUNG, L. A. YOUNG, C. B. OLKIN, AND M. W. BUIE

Southwest Research Institute, 1050 Walnut Street, Boulder, CO 80302; efy@boulder.swri.edu, layoung@boulder.swri.edu,
colkin@boulder.swri.edu, buie@boulder.swri.edu

K. SHOEMAKER

Shoemaker Labs, Inc., 780 Applewood Drive, Lafayette, CO 80026;
shoemakerlabs@gmail.com

R. G. FRENCH

Dept. of Astronomy, Wellesley College, 106 Central Street, Wellesley, MA 02481; rfrench@wellesley.edu

AND

J. REGESTER

Greensboro Day School, 5401 Lawndale Drive, Greensboro, NC 27455; jregester@gmail.com

Received 2009 June 5; accepted 2011 April 21; published 2011 June 16

ABSTRACT. The PHOT (Portable High-Speed Occultation Telescope) systems were developed for the specific purpose of observing stellar occultations by solar system objects. Stellar occultations have unique observing constraints: they may only be observable from certain parts of the globe; they often require a rapid observing cadence; and they require accurate time-stamp information for each exposure. The PHOT systems consist of 14 inch telescopes, CCD cameras, camera mounting plates, GPS-based time standards, and data acquisition computers. The PHOT systems are similar in principle to the POETS systems (Portable Occultation, Eclipse, and Transit Systems), with the main differences being (1) different CCD cameras with slightly different specifications and (2) a standalone custom-built time standard used by PHOT, whereas POETS uses a commercial time standard that is controlled from a computer. Since 2005, PHOT systems have been deployed on over two-dozen occasions to sites in the US, Mexico, Chile, Namibia, South Africa, France, Austria, Switzerland, Australia, and New Zealand, mounted on portable 14 inch telescopes or on larger stationary telescopes. Occultation light curves acquired from the 3.9 m AAT (Anglo-Australian Telescope) have produced photometric signal-to-noise ratios (S/N) of 333 per scale height for a stellar occultation by Pluto. In this article we describe the seven PHOT subsystems in detail (telescopes, cameras, timers, and data stations) and present S/N estimates for actual and predicted occultations as functions of star brightness, telescope aperture, and frame rate.

Online material: color figures

1. INTRODUCTION

1.1. Occultations

An occultation is an event in which one object passes completely behind another object. In a stellar occultation, a star is briefly obscured by a planet or other object. For solid bodies with no appreciable atmosphere or coma, such as an asteroid, an occultation results in the sudden winking out and reappearance of the stellar signal. Observations of a solid-body occultation from multiple sites results in a raster scan of the occulting body, yielding its size, shape, and albedo (e.g., Millis et al. 1987; Dunham et al. 1990; see our Fig. 1). For rings around giant planets or dust jets and comae around comets or centaurs,

occultations measure the line-of-sight transmission along a chord cutting through the system. When a star is occulted by a planetary atmosphere, vertical variation in the atmospheric refractivity defocuses the starlight, providing temperature and density profiles of the obscuring atmosphere that could not be obtained any other way (Fig. 2).

Stellar occultation campaigns have produced a steady stream of major results, including the discovery and characterization of the Uranian rings (Elliot et al. 1977), the discovery of Pluto's atmosphere (Hubbard et al. 1988; Elliot et al. 1989), the super-rotating zonal winds of Titan's atmosphere (Hubbard et al. 1993; Sicardy et al. 1999), the rapidly changing column abundances of Pluto's and Triton's atmospheres (Olkin et al. 1997;

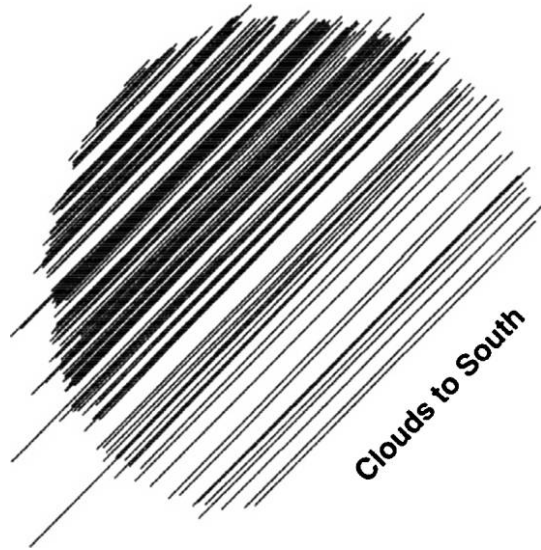


FIG. 1.—Diagram of a stellar occultation by an airless body. Different observing sites probe different parts of the occulting body's shadow as it passes over the Earth. Combining multiple observations produces a raster scan of the object, yielding information on its size and shape. A single chord can only provide a lower limit to the object's radius. This example shows the results of an occultation by Pallas (Dunham et al. 1990).

Elliot et al. 2000; Young et al. 2008), the characterization of gravity waves in the atmospheres of Titan and the gas giants (French & Geirasch 1974; Sicardy et al. 1999), and the refinement of sizes and positions for tens of asteroids per year.

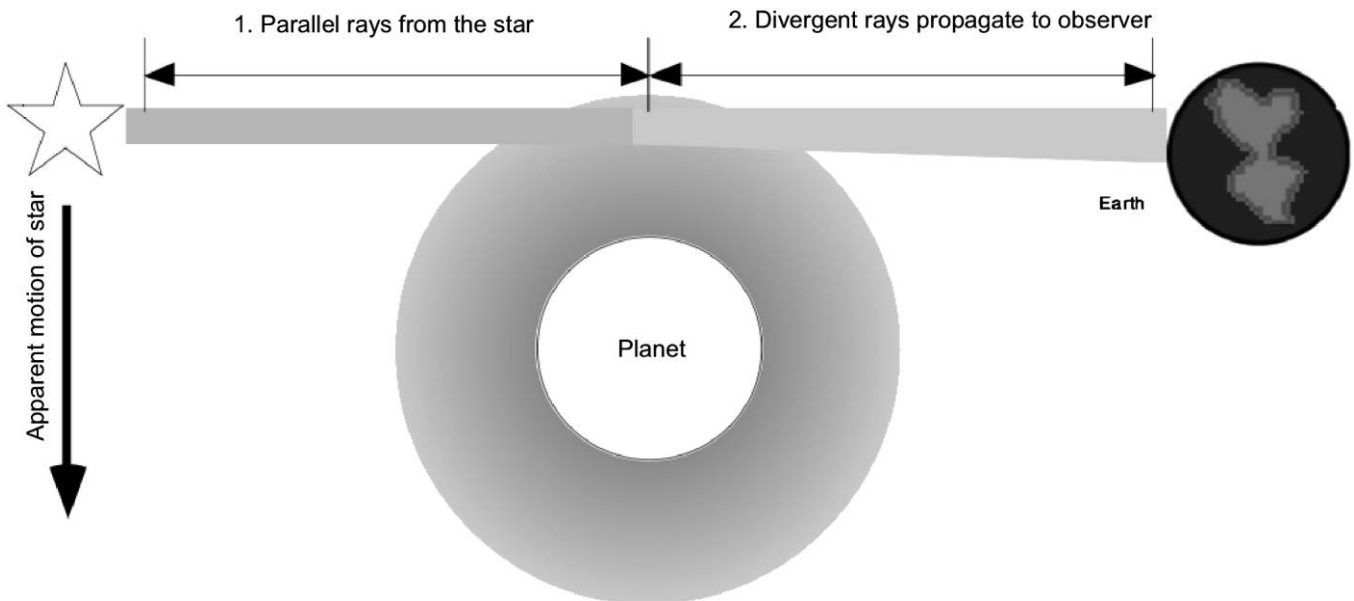


FIG. 2.—Diagram of a stellar occultation by a planetary atmosphere. The star appears to move behind an object due to the relative motions of the Earth, a star, and the occulting object. The star fades during ingress and reappears during egress. Even a clear atmosphere will attenuate starlight before the surface of the occulter is encountered. Because atmospheres are generally thicker at lower altitudes, rays from the star are refracted more if they impact the occulter's atmosphere near the surface. The attenuation due to differential refraction is often more significant than attenuation due to atmospheric opacity by hazes and aerosols. Because of differential refraction, occultations in visible and near-IR wavelengths typically probe down to microbar pressure levels. See the electronic edition of the *PASP* for a color version of this figure.

Because solar system objects have well-known orbital motions, improved time resolution of a stellar occultation observation translates into better spatial resolution of the occulting object. For objects beyond the asteroid belt, the star's relative velocity in the object's sky plane is typically around 20 km s^{-1} , dominated by the Earth's orbital motion, but can be much less if the occultation occurs near the stationary point of the object's orbit. The two main properties of the PHOT design (portability and good signal-to-noise ratio [S/N] at high frame rates) are driven by the need to observe from sites around the world and at a cadence that oversamples the duration of typical occultation events.

The remainder of this article is laid out as follows: § 1.2 describes the design requirements for a portable occultation system, § 2 describes the actual components of the PHOT systems (including cameras, timing systems, data acquisition systems, the telescopes themselves, and provisions for packing and transporting the PHOT systems), and § 3 compares the predicted performance of the PHOT systems with actual performance observed during past occultations.

1.2. PHOT Design Requirements

1.2.1. Frame Rates

What frame rates are needed to characterize the size of an object or an atmosphere's vertical profile? It is reasonable to assume an upper limit for the relative velocity between the occulter and the occulted star of 20 km s^{-1} ; only a subset of

asteroids or near-Earth objects will be faster. Given that relative velocity, a frame rate of 20 Hz will take data at 1 km intervals.

While it would be useful to characterize many phenomena at the 1 km level, other factors can impact the resolution at this level. The angular diameter of the star can be a limiting factor; for the 28 Sgr occultation by Titan, the effective stellar size was estimated to be 20 km. For fainter occultation stars, the stellar size is more typically around 1 km.

The Fresnel diffraction limit is a second limiting factor:

$$\text{Fresnel limit} = \sqrt{\lambda D/2}, \quad (1)$$

where λ is the wavelength of the observation and D is the distance to the occulter. For visible-wavelength events ($\lambda = 700$ nm) at Jupiter's average distance from the Earth, the Fresnel scale is 0.7 km. For infrared ($2.2 \mu\text{m}$) events at 30 AU, the Fresnel scale is 4.45 km.

The scale heights of the atmospheres of Jupiter, Uranus, Titan, and Pluto range from 20 to 60 km. A frame rate of 2 Hz will oversample the scale heights, and faster frame rates will reveal density and temperature perturbations on the scales of a few kilometers. Accordingly, we have chosen frame rates up to 20 Hz as a PHOT design goal, which means that the PHOT cameras must have dead time between frames that is small compared with 0.05 s. Near-zero dead time between exposures is routinely achieved with frame transfer (FT) CCDs. With FT CCDs, the dead time between exposures is the time required to transfer charge from the active region of the CCD to the storage region, typically a few microseconds per parallel shift or a few milliseconds per exposure. The storage region can be read out without disturbing the active region. Provided the readout time is less than the requested exposure time, a sequence of frames can be obtained with only a few milliseconds of dead time between frames.

The readout time is often inversely correlated with the read noise; at the time the PHOT systems were assembled, CCDs with 5–10 MHz readout rates typically had read noises in the $10 e^- \text{ read}^{-1}$ range, while slower rates (e.g., 100 KHz) achieved read noises in the neighborhood of $1\text{--}3 e^- \text{ read}^{-1}$. There are ways to improve the overall frame rate and still reap the benefits of a low read noise system. Consider 100 KHz as a lower limit; at 100 KHz, a 512×512 frame readout would take about 2.5 s, much longer than the target exposure time of 0.1 to 0.05 s. In practice, however, one can usually reduce the number of readout operations per frame by reading subframes around the occultation star and binning pixels in hardware. The disadvantage of reading small subframes is the reduced number of on-chip stars that might be used as photometric standards. Nevertheless, a 128×128 subframe, binned 2×2 , takes just over $0.04 \text{ s frame}^{-1}$ to read at 100 KHz and is compatible with a 20 Hz frame transfer system.

Hardware binning is appropriate when the CCD's plate scale vastly oversamples the seeing. The plate scale is inversely pro-

portional to the telescope's focal length. The shortest focal lengths we have used in 4 yr of PHOT deployments has been 3750 mm on our 14 inch (35 cm) Schmitt-Cassegrain telescopes. This focal length produces a plate scale of $0.055'' \mu\text{m}^{-1}$ (or $0.7'' \text{ pixel}^{-1}$ for our $13 \mu\text{m}$ pixels). This plate scale oversamples the seeing resolution from most (but not all) sites; we would consider binning (2×2) only if the seeing were worse than $2''$ or if there were a need for a wide field of view (FOV) at fast frame rates. If the seeing conditions vary substantially from frame to frame, one might extract a photometrically better light curve using PSF (point-spread function) fitting instead of aperture photometry. In these cases, there is a benefit to oversampling the PSF as part of the PSF-fitting process.

Software binning (after individual pixels have been read out, as opposed to on-chip binning in hardware) is never appropriate. Like hardware binning, it reduces the spatial resolution, but unlike binning in hardware, it provides no improvements in readout time or higher S/N.

1.2.2. Noise Sources

There are many more faint stars than bright ones and many more occultations of faint stars than bright ones. The practical faint-event limit depends on the S/N that can be obtained during an event, which in turn depends on brightness of the occulted star, the occulting object, the maximum acceptable exposure time, the read noise, and the noise from combined background sources:

$$S/N = \frac{S}{\sqrt{rn^2 + S + O + BG}}, \quad (2)$$

where the numerator, S , is the signal (counts from the occulted star in e^-) and the denominator is the noise, which is the quadratic sum of variances due to read noise (rn^2) and photon shot noise from the source (S), the occulter (O), and background sources (BG). Equation (2) assumes that the noise sources are uncorrelated and that all noise terms are in units of electrons. Dark current has never been a significant noise source in any of our occultation campaigns, due to the short exposure times that have been used. In addition to terms in the denominator of equation (2), other systematic noise sources can corrupt a light curve, like variable clouds or scintillation. We always ratio the flux from the occulted star to one or more on-chip comparison stars. The widest FOV used to date with the PHOT systems has been $6'$ (with the 3750 mm focal-length portable 14 inch telescopes), small enough to ensure that the entire FOV is affected similarly by cloud cover, scintillation, and variable seeing.

Although the *variance* in counts from the occulted object O (which is equal to the *counts* from O) might be considered to be part of the background, we have explicitly called it out as a separate noise source to emphasize that the photon shot noise from the occulting object often dominates all other noise sources.

1.2.2.1. Read Noise Versus Photon Shot Noise

When the occulting object and the occulted star are both faint, the dominant noise source is likely to be read noise. This is especially true if the exposure times are short. Since frame rates translate to spatial resolution, exposure times are nearly always as short as possible, up to resolutions corresponding to the Fresnel limit. These objectives dictate the main characteristics of a good occultation detector: high quantum efficiency (QE), high frame rates, low read noise, and zero dead time between exposures.

For faint, read-noise-limited events, low read noise and high QE are the most essential CCD characteristics. For example, consider two cameras that only differ in their read-noise values: one at $3 e^- \text{ read}^{-1} \text{ pixel}^{-1}$ and the other at $10 e^-$. The improvement in S/N due to lower read noise is equivalent to a factor of 10 in exposure times or in occultation star brightness. The camera with $3 e^-$ read noise will be able to sense approximately four times as many events as the $10 e^-$ camera at a given S/N limit.

1.2.2.2. The Case for EMCCDs

CCD vendors have achieved essentially zero-read-noise cameras with electron-multiplying CCDs (EMCCDs). These devices have extended serial registers that amplify the signal from a pixel before it is read by an analog-to-digital converter (ADC). Even if the ADC has a read noise of 10 or $100 e^-$, the effective read noise is nearly zero after dividing by the serial register gain factor. The downside of these devices is that other noise sources are amplified by the serial register by 40% (Robbins & Hadwen 2003), so using an EMCCD is roughly equivalent to halving the size of the aperture and eliminating read noise from the detector. For very faint events, the EMCCD mode can be advantageous, but for cases in which the occulting object is as bright as Pluto, the read noise is overwhelmed by photon shot noise of the sources, even for 14 inch apertures. In § 3.1 we present a S/N calculator and compare the predicted S/N for EMCCD versus conventional CCD modes. EMCCDs also have lower dynamic ranges than conventional readout CCDs. This may not be a factor in occultation observations at high frame rates (e.g., 20 Hz), where all the sources in the frame are read-noise-limited, but could potentially prevent the use of a bright comparison star in some cases.

1.2.3. Detector Sensitivity

Detector sensitivity, or quantum efficiency, is a simple design goal to articulate: we want the QE to be as close to 100% as possible. High QEs are typically achieved by using thinned, back-illuminated CCDs. At the time that the original PHOT cameras were purchased from Roper Scientific (late 2004), the extra step of thinning and back-illumination raised the company's CCD's QEs from around 40% to 90% over the $0.45 \mu\text{m}$ – $0.75 \mu\text{m}$ wavelength range.

1.2.4. Dark Current

Dark current is not a major noise source for most occultations because the exposure times are generally short. Nevertheless, cooled CCDs are available and should be part of the purchase decision, since dark current generally doubles for every 7°C rise in detector temperature. The nominal dark current for the PhotonMax cameras at -55°C is $0.008 e^- \text{ pixel}^{-1} \text{ s}^{-1}$.

Both the MicroMax and PhotonMax CCDs are thermoelectrically cooled, to -45°C and -80°C , respectively. Liquid N_2 systems are also available, but are probably not necessary for occultation observations. One concern with a thermoelectrically cooled system is power consumption, which can be several hundred watts during the initial few minutes of cooldown. The PHOT systems have been run from a car battery, but a powerful inverter (capable of more than 800 W at 110 V) was needed to run the CCD, telescope, laptop, and timer.

1.2.5. Accurate Times and Triggered Exposures

One of the most critical aspects of occultation observations is the need for accurate knowledge of the absolute beginning and end times of each exposure. Occultations are almost always observed from multiple sites, since multiple chords break the degeneracy between uncertainties in the geometry of the event and sought-after physical parameters. Separate data sets need accurate absolute timing if they are to be combined in a useful way. Our requirement for absolute timing accuracy is $500 \mu\text{s}$, corresponding to about 1% of the duration of a 0.05 s exposure.

The need for accurate time stamps leads to the requirement that the camera can be triggered to take each exposure, from an external signal at the transistor-to-transistor (TTL) level, for example. Many cameras can be triggered from a host computer, but it can be difficult to accurately set, verify, and maintain a laptop's internal clock in the field at the millisecond level. For this reason, we require a camera for which each individual exposure can be triggered from a signal with an accurate time pedigree.

We generate triggers with AstroTimers, standalone, custom-designed, and built time standards. These GPS-based units are described in more detail in § 2.2, and the system requirements are shown in Table 1.

2. TECHNICAL DESCRIPTION OF THE PHOT SYSTEMS

2.1. Cameras

The PHOT systems use two different model cameras from Roper Instruments. Four of the PHOT cameras use MicroMAX 512BFT units. Three of the PHOT cameras use PhotonMAX 512B units. Although the PhotonMAX cameras were purchased because the MicroMAX units were no longer available, the two models have distinctive strengths that make them appropriate for different types of events.

TABLE 1
ORIGINAL REQUIREMENTS AND ACTUAL PERFORMANCE OF THE PHOT SYSTEMS

Feature	Goal	Performance of PHOT
Frame rate	1–20 Hz	10 Hz (routine), 20 Hz with a 64×64 subframe
Dead time	<10% of frame rate	<4% of maximum frame rate with frame transfer CCD
Field of view	1–20'	6' with the 14 inch Meade telescopes, 0.4' from the 4 m AAT
Plate scale	0.5–1.2" pixel ⁻¹	0.75" pixel ⁻¹ , 14 inch Meade
Timing knowledge	<1 ms	<1 μ s for 1 PPS, <1 ms for user-defined pulse trains
Deployability	Worldwide, <3 weeks' lead time	2 weeks, typically
Ease of setup	Observe <1 hr after first star acquisition	30 min setup, typically
Sensitivity to Pluto's atmosphere	S/N = 16 at 5 Hz	For $V_{\text{OCC}} = 15.5$, measured S/N per exposure is >20 at 5 Hz with 14 inch Meade or >50 at 10 Hz with 4 m AAT

2.1.1. Common Characteristics

Both cameras have back-illuminated CCDs and high QEs (Fig. 3), thermoelectric cooling, 512×512 pixels, frame transfer operation, capability of using external triggers, subframe readout modes, and hardware binning.

The MicroMAX cameras (Fig. 4) have two ADCs that can be selected via the data acquisition application. These run at 100 KHz and 5 MHz, with read noises of 3.1 and 11 e^- , respectively (the nominal read noise at 100 KHz is 4 e^- , but we measured lower read noises in our laboratory tests). The MicroMAX camera is connected to a data acquisition laptop via a USB 2.0 interface. This common interface allows us to use nearly any laptop on the market that can run Windows XP and WinView, the data acquisition application from Roper Scientific. The MicroMax cameras are about the size and weight of two bricks ($12 \times 12 \times 20$ cm; 7.5 lb). They are run from a separate electronics box that is about the size of a toaster oven and weighs about 20 lb. The MicroMAX cameras are thermoelectrically cooled to about -45°C . There is a vacuum around the CCD assembly that occasionally needs to be pumped down.

The PhotonMAX cameras have two conventional and two EMCCD ADC modes (four total). The conventional modes are at 1 and 5 MHz, with corresponding read noises of 7 and 11 e^- , respectively. The electron multiplication modes are at 5 and 10 MHz, with negligible effective read noises. The PhotonMAX cameras have a factory-sealed vacuum that cannot be pumped (and is supported by a lifetime warranty). They are thermoelectrically cooled to -80°C . The PhotonMAX cameras are slightly bigger than the MicroMAX CCD head units but have no separate electronics boxes. The PhotonMAX data rates are too fast for USB 2.0; they interface to a data acquisition computer via a half-height PCI card. The PHOT systems use Dell D620 laptops with docks to host the half-height cards.

2.2. Timers

We designed and built two generations of AstroTimers. Both are based on GPS chips that were specifically intended to provide accurate times. The GPS chips provide the following:

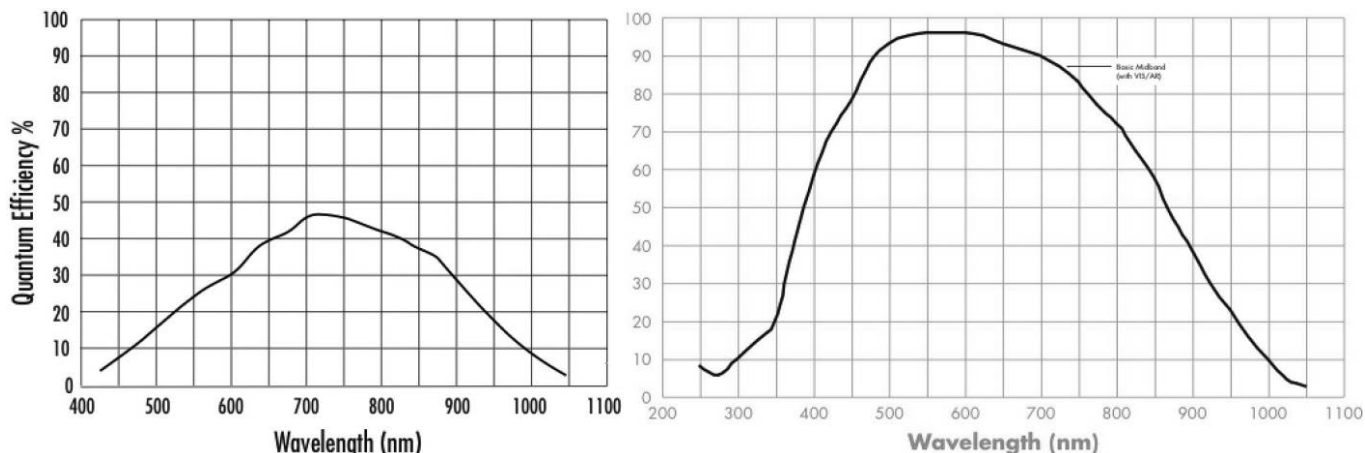


FIG. 3.—QE curves for the Roper MicroMax 512FT (left) and MicroMax 512BFT (right). The BFT designation means that the detector is a thinned, back-illuminated, frame-transfer CCD. The advantage over a nonthinned, non-back-illuminated CCD is more than a factor-of-2 increase in QE.



FIG. 4.—The MicroMax 512BFT camera (*left*) and the PhotonMax 512B camera (*right*).

1. National Marine Electronics Association strings with latitude, longitude, altitude, time, number of satellites being tracked, and dilution of precision (a measure of the accuracy of the position/time solution).

2. A 1 PPS (pulse-per-second) output, consisting of a TTL signal with a rising edge every second. The nominal accuracy of this PPS signal is 30–70 ns, according to NavSync (the GPS chip manufacturer) literature.

3. A variable frequency output, synched to the PPS signal, user-selectable from 10 KHz to 10 MHz. We use the GPS chip-set's 10 KHz output to generate user-definable signal trains. The AstroTimer's pulse-counting subroutines impose a delay of 1.3 ms to these signal trains, but this delay is a measured quantity that varies by less than 0.1 ms.

Both AstroTimers use two or more single-board computers (SBCs) from Vesta Technology, Inc. (Fig. 5). The main purpose of the SBC is to generate triggers in the form of a signal train from the 10 KHz output of the GPS chip. In the first-generation AstroTimers, the user specifies a start time, a pulse interval and pulse duration, and number of pulses to generate. One SBC is dedicated to counting 10 KHz pulses and generating the requested sequence of pulses. Two other SBCs are dedicated to (1) providing a user interface via a 16-character keyboard and (2) updating a display of the UT time.

The second-generation AstroTimers are simpler than the first-generation units. They lack the ability to preprogram the start time. Instead, the pulse train begins on an integer second shortly after the user flips a switch. The exact start time is displayed when the sequence of pulses begins. The second-generation AstroTimers use a single SBC to count 10 KHz pulses and generate the signal train, and they provide a user interface via push buttons and toggle switches.

The second-generation AstroTimers use a CW12-TIM GPS receiver model manufactured by NavSync. This module is a small ($40 \times 60 \times 10$ mm) board. The rms error on the 1 PPS output is rated at 30 ns. The nominal time for a typical cold start is 45 s.

The ability to generate a specific number of triggers (and no more) has turned out to be an important feature. The data col-

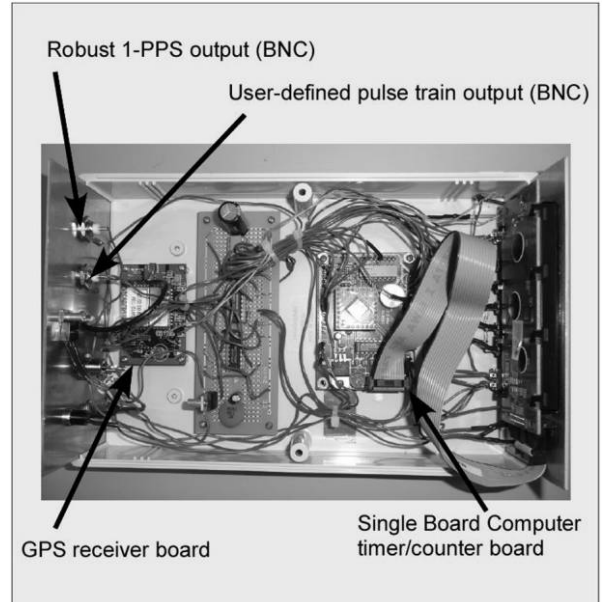


FIG. 5.—Inside the GPS-based AstroTimer. Outside dimensions are $6'' \times 10'' \times 3''$. See the electronic edition of the *PASP* for a color version of this figure.

lection software can also be programmed to collect a certain number of images. If, after an AstroTimer has generated N pulses, the data collection software reports that fewer than N exposures were triggered, then we know that some triggers were missed. In practice, we have never lost triggers in any deployments.

Both versions of AstroTimers run off of 12 V DC. Both have SMA connectors to GPS antennas. Both have BNC connectors to (1) PPS output and (2) the user-specified pulse train. The PPS output comes directly from the GPS chip. It is intended to provide some basic triggering capability in the event of a malfunction of an SBC.

2.3. Telescopes and Mounts

2.3.1. The Portable 14 Inch Telescopes

The choice of 14 inch telescopes was a compromise between the opposing goals of (1) maximizing the S/N during an occultation and (2) maintaining the portability of the telescope. The PHOT systems include four 14 inch Meade Schmidt-Cassegrain telescopes. These telescopes have a focal length of 3750 mm in a relatively compact form. The combined weight of the tripod, fork mount, and optical tube assembly is about 190 lb.

At the time that these telescopes were purchased, there were telescopes of similar aperture being sold by competing vendors. Except for the altitude-azimuth (alt-az) Meade telescopes, all comparable telescopes used German equatorial mounts and were therefore unacceptable for occultation work. German equatorial mounts cannot track an object as its hour angle crosses



FIG. 6.—A PHOT camera (MicroMax 512BFT) mounted on the auxiliary port of the 3.9 m AAT. Shown here are the MicroMax CCD head unit (a), the cable (b) connecting it to the electronics box, the aluminum standoffs to which the camera is bolted (c), and an adapter plate (d) with a bolt hole pattern to mate the standoff unit to the telescope.

zero without stopping to move the telescope over the pier. The ability of the telescope to track objects across the sky without interruption was an essential requirement for occultation observations. The chief disadvantage of alt-az systems, the need for an image rotator for long exposures, is not relevant to occultation work. (Even with image rotation, it is a simple matter to identify the approximate positions of the occultation star and the comparison stars—sometimes we use known offsets [and known rotation angles] from the brightest star in the frame. Once the approximate positions are known, our photometry pipeline determines subpixel centroids for stars and extracts their fluxes).

The alt-az drive of the Meade 14 inch telescopes was the deciding factor in choosing a portable telescope. In addition, the Meade telescopes have go-to electronics that vastly simplify

TABLE 2
SIZE AND WEIGHT OF COMPONENTS

Component	Size (packed) (inch)	Weight (lb)
Detector	5 × 5 × 8	8
CCD controller	6 × 9 × 13	20
Laptop	1 × 9 × 11	7
Dock	3 × 19 × 16	8
GPS time standard	2 × 6 × 9	3
Optical tube assembly and mount	17 × 26 × 38	160
Tripod	48 × 12 × 12	50
Field kit (tools and parts)	6 × 8 × 14	25
Telescope case (JMI)	20 × 25 × 48	45
Camera and laptop case	18 × 20 × 24	12
Total		338

TABLE 3
COMPONENT POWER REQUIREMENTS

Component	Power requirements	Power source(s)
Camera	300 W ^a	120–240 V AC or car ^b
Laptop (with dock)	90 W	120–240 V AC or car ^b
AstroTimer	10 W	12 V DC
Telescope	1 W	12 V DC or 8 C-cell batteries

^a The power drawn by the CCD during the initial cooldown phase can exceed 300 W. When running the MicroMax CCDs from a car battery, an 800 W (or greater) inverter was required during the cooldown period.

^b “Car” means a 120 V AC inverter powered from a car-battery/cigarette lighter. On past observing runs, the telescope, camera, laptop, and AstroTimer were all powered from a car (with the engine running) and an 800 W inverter.

finding the occultation field. Finally, the telescopes can run on eight C-cell batteries or on 12 V DC.

2.3.2. PHOT Systems on Large Telescopes

Most of the PHOT deployments have been used on fixed telescopes at existing observatories. Although many facilities already have visible-wavelength cameras, the advantages of the PHOT cameras (low read noise, high QE, virtually no dead time, high frame rates, and precise time-stamping) have proved

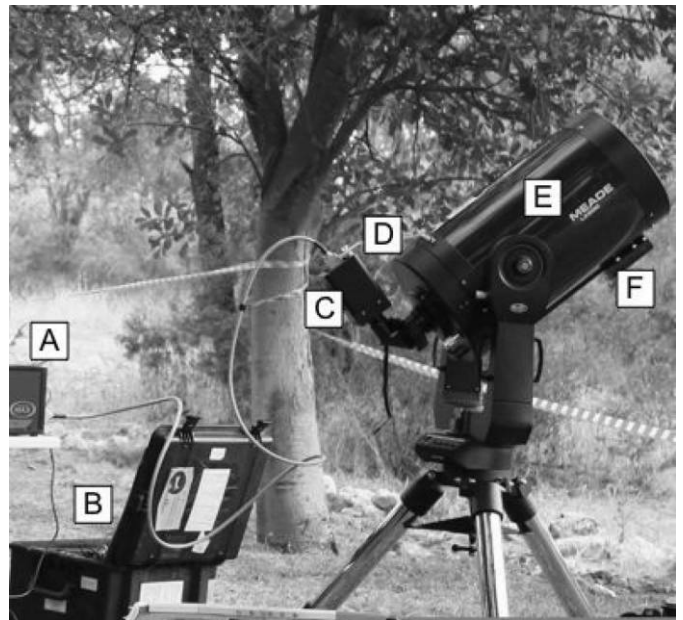


FIG. 7.—A PHOT system deployed in Namibia in 2009 April showing the following components: the MicroMax camera electronics box (a), the Hardigg foam case for the MicroMax camera and the AstroTimer (b), the MicroMax CCD head unit (c), a strain-relief bracket for the CCD (d), a 14 inch Meade telescope (e), and third-party counterweights (f). See the electronic edition of the *PASP* for a color version of this figure.

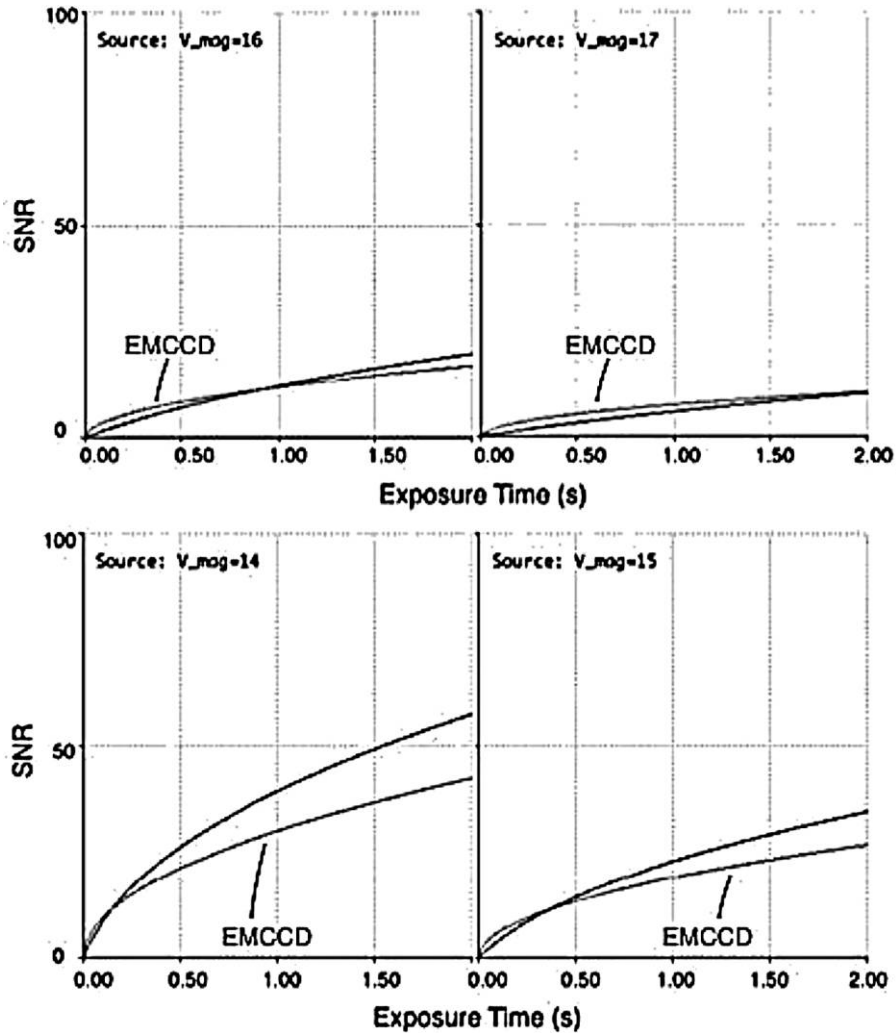


FIG. 8.—S/N Estimates for 14 inch Meade/MicroMax 512BFT PHOT Systems. S/N estimates for exposure times between 0 and 2 s for a PhotonMax 512B camera in EMCCD mode and a MicroMAX 512BFT camera with $3.1 e^-$ read noise. Four source brightnesses are considered ($V = 14, 15, 16,$ and 17), where the source brightness refers to the combined signal from the occulting object and the occulted star. As expected, the EMCCD has an advantage when there is not much light (i.e., for faint sources and/or short exposure times). For a $V = 16$ source (about four times fainter than Pluto), the crossover point is at 1 s. EMCCD mode is less advantageous at telescopes with apertures larger than 14 inch.

to be worth the effort of transporting and mounting the cameras on fixed telescopes.

We have built adapters for both types of cameras that add a short 2 inch (50.4 mm) outer-diameter tube to the front of the CCD, centered on the active region of the CCD. This “snout” adapter lets us easily mount the cameras to telescopes that already accept 2 inch eyepieces. We have also machined adapter plates to interface to many different telescopes, such as the AAT (Fig. 6).

2.4. Data Acquisition

Roper Scientific distributes an application, WinView, to run their MicroMax and PhotonMax cameras. They also distribute a

cross-platform library, PVCam, for development of data acquisition applications on Macintosh, Windows, and Linux platforms. While it would be nice to write a program tailored to occultation observations, we have found WinView to be adequate. It allows the user to specify hardware binning, subframe location, and hardware triggering, all of which are necessary for our occultation runs.

We use laptops running Windows XP Professional as data acquisition stations. The MicroMax cameras can be operated from virtually any PC with a USB 2.0 port. Because the PhotonMax data rate has a significantly higher ceiling, those cameras interface to the host computer via a half-height PCI card. We run the PhotonMax cameras from Dell Latitude D620 laptops

TABLE 4
MAGNITUDES AND OBSERVED DATA NUMBERS FOR STARS IN
FIG. 10

Star label	DN ^a	UCAC mag ^b	UCAC2 identification
A	25	15.0	26039859
B	76	13.2	26039956
C	14	15.2	26039936
D	107	13.5	26039894
E	24	14.2	26039875
F	31	14.3	26039845
G	19	14.7	26039867
H	46	13.7	26039844

^aBackground-subtracted counts per 0.5 s exposure.
^bFrom 579–642 nm.

connected to docking stations that have the Roper PCI cards installed.

The data acquisition laptops are typically within 15 ft of the camera or electronics box, constrained by the length of a USB or data cable. On large telescopes, we often have to fix the acquisition laptop to the telescope structure and provide access to the laptop from a distant control room. There are several ways to control a laptop remotely; we most often use virtual network computing (VNC) for this purpose. The acquisition laptop is either connected to a network via Ethernet or WiFi, or a long Ethernet cable is used to directly connect the control-room computer to the laptop. The time lag of the VNC connection has not been an obstacle in any of our observing campaigns.

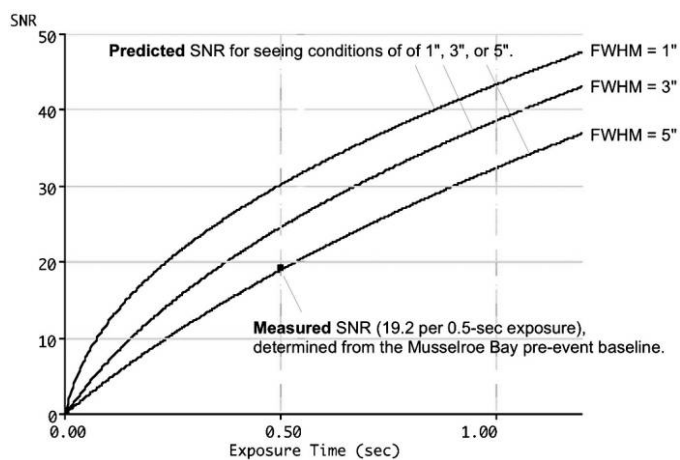


FIG. 9.—Predicted and actual performances of a PHOT system on a 14 inch telescope. For small telescopes and faint sources, the S/N is a sensitive function of the seeing and focus quality. This is expected: poor seeing means that point sources are spread over more pixels, resulting in a higher read-noise penalty when a source's counts are summed over all those pixels. At the Musselroe Bay site (2007 July 31), the measured S/N was comparable with the predicted S/N under the assumption that the typical source FWHM was around 4–5", which is consistent with the image quality from that night.

2.5. Packing and Transport

Telescopes are transported in wheeled, foam-lined fiberglass cases from JMI Telescopes (Jim's Mobile, Inc., Golden, Colorado) that are sold specifically for the 14 inch Meade telescopes. These cases are sufficient for transport within a car, but not for shipping. In 2006 we had two wooden cases built by Crating Technologies (Longmont, Colorado) to contain the JMI cases and tripods. (Wood used in internationally shipped crates has to be certified for that purpose.)

The total round-trip cost of shipping a telescope (including carnets or other customs documents, shipping containers, etc.) to distant international destinations has been close to \$3000, or about half the cost of the telescope itself. For that reason, we have decided to leave one telescope in Tasmania for future Southern Hemisphere events.

The PHOT cameras, laptops, and AstroTimers can be checked as luggage in padded cases made for us by Atlas Case Corp. (Denver, Colorado). We use Pelican-Hardigg cases (model iM2750), with foam cutouts for cameras, laptops, docks (for the PhotonMax cameras), AstroTimers, and cables (see Tables 2

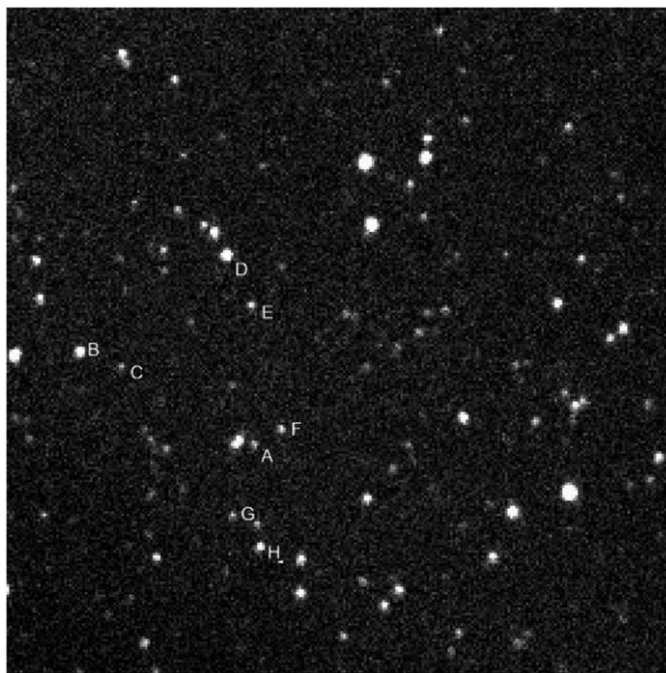


FIG. 10.—Observed counts for faint stars using PHOT. In this 0.5 s exposure of the 2006 June 12 Pluto occultation field (obtained with a 14 inch Meade telescope from the Campbell Farm in Longford, Tasmania), we have extracted counts for eight faint stars to demonstrate the sensitivity of the PHOT cameras. The occultation star, A, has an estimated USNO CCD Astrograph Catalog magnitude (between *V* and *R* filters) of 15.0 and generated 811 DN (data number, or counts) in this image. Given the gain (about $2 e^- \text{DN}^{-1}$), the background noise level (about $18 e^- \text{pixel}^{-1}$), the FWHM (about 2.1 pixels), and the read noise (about $3.1 e^- \text{pixel}^{-1}$), the measured S/N of star A is 2.5 in a 0.5 s exposure. Without the high background (which roughly doubled the noise from other sources), the S/N would have been 6.4 per 0.5 s exposure. See Table 4 for the UCAC magnitudes, CCD counts (in DN), and UCAC2 ID numbers.

and 3). The weight of the case alone is about 18 lb; the loaded cases are close to 48 lb, just under the 50 lb oversize limit currently imposed by many airlines. (Fig. 7)

3. EVALUATION OF THE PHOT SYSTEMS

In this section we try to address two questions: What is the predicted performance of the PHOT systems? How have the PHOT systems lived up to these predictions?

3.1. Predicted S/N

We have written S/N estimators to help compare cameras with different characteristics, to compare binning factors, and to decide how fast of a cadence will be possible for an event of a given brightness. Figure 8 shows predicted S/N given the following assumed parameters: sky $V_{\text{mag}} = 22.5$, point-source FWHM = 2.0, telescope aperture is 14 inch, clear aperture is 87.6% (a 4.9 inch [12.3 cm] secondary), telescope transmission at 750 nm is 83% (for Meade's UHTC optics), read noise for the MicroMAX 512BFT camera is $3.1 e^-$, read noise for the PhotonMAX 512B EMCCD camera is effectively zero, and PhotonMAX 512B excess noise factor in EMCCD mode for noise sources other than read noise is 1.4.

3.2. Performance from Past Deployments

This section compares predicted versus observed performances for two previous Pluto occultations: one that used a MicroMax 512BFT 14 inch telescope (from a 2007 July 31 event observed from Tasmania; see Fig. 10 and Table 4) and another that used a MicroMax 512BFT camera mounted on the 4 m AAT (from the 2006 June 12 event observed from

Siding Spring). These two cases are end members (in aperture) among the roughly two-dozen deployments that have been undertaken to date with PHOT cameras.

The 2007 July 31 event was observed from Musselroe Bay in Tasmania. This event illustrates that the value of a portable telescope can outweigh the effort and expense associated with its shipment and operation. This telescope provided an important chord across Pluto's shadow path in a region that did not have fixed telescopes of a comparable aperture, but more significantly, the observers (in consultation with the local branch of the Australian Bureau of Meteorology) were able to pick a location that had the best prediction for clear skies. In contrast, observers at the Mount Canopus Observatory in Hobart had significant cloud cover through most of the event. The occulted star was labeled P495.3 on our internal watch lists; it was a moderately fast event (sky-plane velocity of 16.4 km s^{-1}) and relatively bright (V_{mag} of 13.25). The predicted versus observed performances of the PHOT system on a 14 inch telescope are shown in Figure 9.

The 2006 June 12 event was observed from the 3.9 m AAT in Siding Spring, Australia. The unfiltered magnitude of the occultation star (P384.2 in McDonald and Elliot 2000a, 2000b) was measured to be 0.83 mag fainter than Pluto on the night of the event (about a V_{mag} of 15), with a sky-plane velocity of 24.0 km s^{-1} . The predicted versus observed performances of the PHOT system on a 3.9 m telescope are shown in Figure 11.

4. SUMMARY AND CONCLUSIONS

The PHOT systems' requirements (Table 1) were originally intended to enable observations of stellar occultations by Pluto or Triton from sites around the world. A PHOT system was first deployed to South America in 2005 to observe a stellar occultation by Charon, with excellent results. Since then, PHOT systems have been deployed over two-dozen times, on telescopes ranging from the 14 inch Meade to the 200 inch (5 m) telescope at Palomar. In 2006, a PHOT system mounted on the AAT obtained the best (highest S/N) Pluto occultation light curve to date, providing evidence of gravity waves in Pluto's atmosphere, the relative lengths of dynamical versus radiative time-scales, the bulk extent of Pluto's atmosphere, evidence for a nonisothermal profile in Pluto's upper atmosphere, and evidence for a temperature inversion (as opposed to a haze layer) to explain the drop in transmission through Pluto's lower atmosphere (Young et al. 2008).

The performance of the PHOT systems has been well characterized (Figs. 9 and 11). We are able to predict the S/N for an event with good accuracy and choose optimum frame rates and binning factors in advance.

In general, the PHOT systems meet or exceed the requirements outlined in Table 1. They have been deployed to international destinations (e.g., to Tasmania or Namibia) with as little as 3 weeks' lead time (if a 14 inch Meade telescope has to be shipped) or 2 days' lead time if only the cameras, AstroTimers,

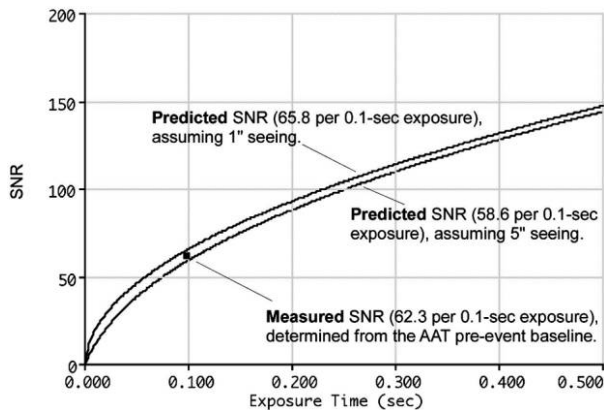


FIG. 11.—Predicted and actual performances of a PHOT system on the 3.9 m AAT. For large telescopes, the quality of the focus or seeing barely affects the S/N of the reduced light curve. Because the read noise is a small component of the total noise, the number of pixels covered by each source only makes a small difference to the total noise estimate. In this case, the measured noise (determined from the flat, pre-event portion of the light curve) was 62.3 for each 0.1 s time step, close to the S/N predictions for seeing conditions between 1 and 5".

and laptops are necessary. We are currently building a prototype of an airline-checkable 22 inch (55 cm), 100 lb telescope. This telescope would reduce the lead time for deployment to most of the globe to 2 days, albeit with possible charges for excess baggage.

The equipment and work described in this article were supported by the National Science Foundation's Major Research Instrumentation Program and NASA's Planetary Astronomy Program. The authors wish to acknowledge an anonymous reviewer for valuable comments and corrections.

REFERENCES

- Dunham, D. W., et al. 1990, *AJ*, 99, 1636
- Elliot, J. L., Dunham, E., & Mink, D. 1977, *Nature*, 267, 328
- Elliot, J. L., Dunham, E. W., Bosh, A. S., Slivan, S. M., Young, L. A., Wasserman, L. H., & Millis, R. L. 1989, *Icarus*, 77, 148
- Elliot, J. L., et al. 2000, *Icarus*, 148, 347
- French, R. G., & Gierasch, P. J. 1974, *J. Atmos. Sci.*, 31, 1707
- Hubbard, W. B., Hunten, D. M., Dieters, S. W., Hill, K. M., & Watson, R. D. 1988, *Nature*, 336, 452
- Hubbard, W. B., et al. 1993, *Icarus*, 103, 215
- McDonald, S. W., & Elliot, J. L. 2000, *AJ*, 119, 1999
- . 2000, *AJ*, 120, 1599 (erratum 119 1999 [2000])
- Millis, R. L., Wasserman, L. H., & French, R. G. 1987, *Icarus*, 69, 176
- Olkin, C. B., et al. 1997, *Icarus*, 129, 178
- Robbins, M. S., & Hadwen, B. J. 2003, *IEEE Trans. Electron Devices*, 50, 1227
- Sicardy, B., et al. 1999, *Icarus*, 142, 357
- Souza, S. P., Babcock, B. A., Pasachoff, J. M., Gulbis, A. A. S., Elliot, J. L., Person, M. J., & Gangestad, J. W. 2006, *PASP*, 118, 1550
- Young, E. F., et al. 2008, *AJ*, 136, 1757